Pergamon

PII: S0022-4073(98)00008-9

CAPABILITIES AND LIMITATIONS OF A CURRENT FORTRAN IMPLEMENTATION OF THE *T*-MATRIX METHOD FOR RANDOMLY ORIENTED, ROTATIONALLY SYMMETRIC SCATTERERS

MICHAEL I. MISHCHENKO† and LARRY D. TRAVIS

NASA Goddard Institute for Space Studies, 2880 Broadway, New York, New York 10025, U.S.A.

Abstract—We describe in detail a software implementation of a current version of the *T*-matrix method for computing light scattering by polydisperse, randomly oriented, rotationally symmetric particles. The FORTRAN *T*-matrix codes are publicly available on the World Wide Web at http://www.giss.nasa.gov/~crmim. We give all necessary formulas, describe input and output parameters, discuss numerical aspects of *T*-matrix computations, demonstrate the capabilities and limitations of the codes, and discuss the performance of the codes in comparison with other available numerical approaches. Published by Elsevier Science Ltd.

1. INTRODUCTION

The *T*-matrix method is a powerful exact technique for computing light scattering by nonspherical particles based on numerically solving Maxwell's equations. Although the method is, potentially, applicable to any particle shape, most practical implementations of the technique pertain to bodies of revolution. The method was initially developed by Waterman[1] and has been significantly improved as described in Refs. 2–6. Specifically, Refs. 4 and 6 extend the method to much larger size parameters and aspect ratios, Ref. 2 presents an efficient analytical procedure for computing the scattering properties of randomly oriented particles, Ref. 3 describes an automatic convergence procedure convenient in massive computer calculations for particle polydispersions, and Ref. 5 presents benchmark *T*-matrix computations for particles with non-smooth surfaces (finite circular cylinders). A general review of the *T*-matrix method can be found in Ref. 7.

In this paper we provide a detailed description of modern *T*-matrix FORTRAN codes which incorporate all recent developments, are publicly available on the World Wide Web, and are, apparently, the most efficient and powerful tool for accurately computing light scattering by randomly oriented rotationally symmetric particles. For the first time, we collect in one place all necessary formulas, discuss numerical aspects for *T*-matrix computations, describe the input and output parameters, and demonstrate the capabilities and limitations of the codes. The paper is intended to serve as a detailed user guide to a versatile tool suitable for a wide range of practical applications. We specifically target the users who are interested in practical applications of the *T*-matrix method rather than in details of its mathematical formulation.

2. BASIC DEFINITIONS

The single scattering of light by a small-volume element dv consisting of randomly oriented, rotationally symmetric, independently scattering particles is completely described by the ensemble-averaged extinction, C_{ext}, and scattering, C_{sca}, cross sections per particle and the dimensionless

---

† Author to whom correspondence should be addressed.

Stokes scattering matrix[8, 9]

$$F(\Theta) = \begin{bmatrix} a_1(\Theta) & b_1(\Theta) & 0 & 0 \\ b_1(\Theta) & a_2(\Theta) & 0 & 0 \\ 0 & 0 & a_3(\Theta) & b_2(\Theta) \\ 0 & 0 & -b_2(\Theta) & a_4(\Theta) \end{bmatrix}, \tag{1}$$

where Θ is the scattering angle, i.e., the angle between the incident and scattered beams. The scattering matrix describes the transformation of the Stokes vector of the incident beam, I^{inc}, into the Stokes vector of the scattered beam, F^{sca}, provided that both Stokes vectors are defined with respect to the scattering plane (plane through the incident and the scattered beams):

$$I^{sca} = \frac{C_{sca}n_0 dv}{4\pi R^2} F(\Theta) I^{inc}, \tag{2}$$

where n_0 is the particle number density, and R is the distance from the small-volume element to the observation point. The Stokes vector is defined as a (4×1) column having the Stokes parameters $I, Q, U,$ and V as its components as follows:

$$I = \begin{bmatrix} I \\ Q \\ U \\ V \end{bmatrix}. \tag{3}$$

The definition of the Stokes parameters can be found in Refs. 8 and 9. Only eight elements of the scattering matrix are nonzero and only six of them are independent. Furthermore, there are special relations for the scattering angles 0 and π:[8,10]

$$a_2(0) = a_3(0), \qquad a_2(\pi) = -a_3(\pi), \tag{4}$$

$$b_1(0) = b_2(0) = b_1(\pi) = b_2(\pi) = 0, \tag{5}$$

$$a_4(\pi) = a_1(\pi) - 2a_2(\pi). \tag{6}$$

The (1,1)-element of the scattering matrix, $a_1(\Theta)$, is the well-known phase function satisfying the normalization

$$\frac{1}{2} \int_0^\pi d\Theta \sin \Theta \, a_1(\Theta) = 1. \tag{7}$$

The quantity

$$g = \langle \cos \Theta \rangle = \frac{1}{2} \int_{-1}^1 d(\cos \Theta) a_1(\Theta) \cos \Theta \tag{8}$$

is called the asymmetry parameter of the phase function and is positive for particles that scatter predominantly in the forward direction, negative for backscattering particles, and zero for symmetric phase functions with $a_1(\pi - \Theta) = a_1(\Theta)$. The ensemble-averaged absorption cross section per particle is defined as the difference between the extinction and scattering cross sections,

$$C_{abs} = C_{ext} - C_{sca}. \tag{9}$$

The probability that a photon incident on a small-volume element survives is equal to the ratio of the scattering and extinction cross sections and is called the single-scattering albedo ϖ:

$$\varpi = C_{sca}/C_{ext}. \tag{10}$$

In computations for rotationally symmetric particles in random orientation, an efficient approach is to expand the elements of the scattering matrix as follows:[2,11]

$$a_1(\Theta) = \sum_{l=0}^{l_{max}} \alpha_1^l P_{00}^l(\cos \Theta), \tag{11}$$

$$a_2(\Theta) + a_3(\Theta) = \sum_{l=2}^{l_{max}} (\alpha_2^l + \alpha_3^l) P_{22}^l(\cos \Theta),\tag{12}$$

$$a_2(\Theta) - a_3(\Theta) = \sum_{l=2}^{l_{max}} (\alpha_2^l - \alpha_3^l) P_{2,-2}^l(\cos \Theta),\tag{13}$$

$$a_4(\Theta) = \sum_{l=0}^{l_{max}} \alpha_4^l P_{00}^l(\cos \Theta),\tag{14}$$

$$b_1(\Theta) = \sum_{l=2}^{l_{max}} \beta_1^l P_{02}^l(\cos \Theta),\tag{15}$$

$$b_2(\Theta) = \sum_{l=2}^{l_{max}} \beta_2^l P_{02}^l(\cos \Theta),\tag{16}$$

where $P_{mn}^l(x)$ are generalized spherical functions,[12,13] and the upper summation limit, l_{max}, depends on the desired numerical accuracy of the expansions. Knowledge of the expansion coefficients α_1^l to β_2^l in Eqs. (11)–(16) allows an easy calculation of the elements of the scattering matrix for essentially any number of scattering angles with minimal computer time. Thus, instead of specifying the elements of the scattering matrix for a large number of scattering angles and using interpolation to calculate the scattering matrix in intermediate points, one can use a limited (and often small) number of numerically significant expansion coefficients. This also makes the expansion coefficients especially convenient in ensemble averaging: instead of computing ensemble-averaged scattering matrix elements for a dense grid of scattering angles, one can average a relatively small number of expansion coefficients. Another advantage of expansions (11)–(16) is that they enable the use of the addition theorem for generalized spherical functions in an efficient calculation of the Fourier components of the phase matrix appearing in the Fourier azimuthal decomposition of the vector radiative transfer equation.[11,14]

Since $P_{00}^l(x) = P_l(x)$, Eq. (11) is the well-known expansion of the phase function in Legendre polynomials widely employed in the scalar radiative transfer theory.[15–18] Using the orthogonality property of generalized spherical functions, we easily derive

$$\langle \cos \Theta \rangle = \alpha_1^1/3.\tag{17}$$

3. T-MATRIX ANSATZ

Consider scattering of a plane electromagnetic wave by a single nonspherical particle in a fixed orientation with respect to the reference frame. In the framework of the T-matrix approach, the incident and the scattered fields are expanded in vector spherical functions M_{mn} and N_{mn} as follows:[19]

$$E^{inc}(R) = \sum_{n=1}^{n_{max}} \sum_{m=-n}^{n} [a_{mn}\mathrm{Rg}M_{mn}(kR) + b_{mn}\mathrm{Rg}N_{mn}(kR)],\tag{18}$$

$$E^{sca}(R) = \sum_{n=1}^{n_{max}} \sum_{m=-n}^{n} [p_{mn}M_{mn}(kR) + q_{mn}N_{mn}(kR)], \quad |R| > r_0,\tag{19}$$

where r_0 is the radius of a circumscribing sphere of the scattering particle, and the origin of the coordinate system is assumed to be inside the particle. Owing to the linearity of Maxwell's equations and boundary conditions, the relation between the scattered field coefficients p_{mn} and q_{mn} on one hand and the incident field coefficients a_{mn} and b_{mn} on the other hand is linear and is given by a transition matrix (or T matrix) T:[1,19]

$$p_{mn} = \sum_{n'=1}^{n_{max}} \sum_{m'=-n'}^{n'} [T_{mnm'n'}^{11} a_{m'n'} + T_{mnm'n'}^{12} b_{m'n'}],\tag{20}$$

$$q_{mn} = \sum_{n'=1}^{n_{max}} \sum_{m'=-n'}^{n'} [T_{mnm'n'}^{21} a_{m'n'} + T_{mnm'n'}^{22} b_{m'n'}].\tag{21}$$

In a compact matrix notation, Eqs. (20) and (21) can be rewritten as

$$\begin{bmatrix} p \\ q \end{bmatrix} = T \begin{bmatrix} a \\ b \end{bmatrix} = \begin{bmatrix} T^{11} & T^{12} \\ T^{21} & T^{22} \end{bmatrix} \begin{bmatrix} a \\ b \end{bmatrix}. \tag{22}$$

Equation (22) forms the basis of the T-matrix approach. Since the expansion coefficients a_{mn} and b_{mn} of the incident plane wave can be easily calculated using closed-form analytical expressions, the knowledge of the T matrix for a given scatterer allows the computation of the scattered field via Eqs. (19)–(21) and, ultimately, the computation of all scattering characteristics introduced in the previous section. A fundamental feature of the T-matrix approach is that the elements of the T matrix are independent of the incident and scattered fields and depend only on the shape, size parameter, and refractive index of the scattering particle as well as on its orientation with respect to the reference frame. Consequently, the T matrix need be computed only once and then can be used in computations for any directions of light incidence and scattering.

Furthermore, it turns out that the T matrix computed for an arbitrary orientation of a nonspherical particle can be directly used in an analytical computation of the scattering characteristics of randomly oriented particles.[2] For example, the extinction and scattering cross sections averaged over the uniform orientation distribution of a nonspherical particle are given by the following simple formulas:

$$C_{ext} = -\frac{2\pi}{k^2} \operatorname{Re} \sum_{n=1}^{n_{max}} \sum_{m=-n}^{n} [T^{11}_{mnmn} + T^{12}_{mnmn}], \tag{23}$$

$$C_{sca} = \frac{2\pi}{k^2} \sum_{n=1}^{n_{max}} \sum_{n'=1}^{n_{max}} \sum_{m=-n}^{n} \sum_{m'=-n'}^{n'} \sum_{i=1}^{2} \sum_{j=1}^{2} |T^{ij}_{mnm'n'}|^2. \tag{24}$$

Similar, albeit less simple analytical formulas exist for the expansion coefficients appearing in Eqs. (11)–(16). One, therefore, does not have to numerically integrate the optical cross sections and the scattering matrix elements by putting a particle in many discrete orientation, as done in Refs. 20–22. Instead, the T matrix can be computed for a single, arbitrarily chosen particle orientation and then used in the analytical averaging procedure developed in Ref. 2. Direct numerical checks suggest that the analytical approach can be faster than the method of numerical orientation integrations by a factor of several tens.[2,23]

The standard scheme for computing the T-matrix for a nonspherical particle is based on the extended boundary condition method (EBCM).[1,24] In addition to the expansions of the incident and scattered fields given by Eqs. (18) and (19), the internal field is also expanded in vector spherical functions:

$$E^{int}(R) = \sum_{n=1}^{n_{max}} \sum_{m=-n}^{n} [c_{mn} \operatorname{Rg} M_{mn}(m_r kR) + d_{mn} \operatorname{Rg} N_{mn}(m_r kR)], \tag{25}$$

where m_r is the refractive index of the particle relative to that of the surrounding medium. The relation between the expansion coefficients of the incident and internal fields is linear and is given by

$$\begin{bmatrix} a \\ b \end{bmatrix} = \begin{bmatrix} Q^{11} & Q^{12} \\ Q^{21} & Q^{22} \end{bmatrix} \begin{bmatrix} c \\ d \end{bmatrix}, \tag{26}$$

where the elements of the matrix Q are two-dimensional integrals which must be numerically evaluated over the particle surface and depend on the particle size, shape, refractive index, and orientation. The scattered field coefficients are expressed in the internal field coefficients as

$$\begin{bmatrix} p \\ q \end{bmatrix} = - \begin{bmatrix} \operatorname{Rg} Q^{11} & \operatorname{Rg} Q^{12} \\ \operatorname{Rg} Q^{21} & \operatorname{Rg} Q^{22} \end{bmatrix} \begin{bmatrix} c \\ d \end{bmatrix}, \tag{27}$$

where, again, the elements of the $\operatorname{Rg} Q$ matrix are two-dimensional integrals over the particle surface. Comparing Eqs. (26) and (27) with Eq. (22), we finally derive

$$T = -\operatorname{Rg} Q[Q]^{-1}. \tag{28}$$

General formulas for computing the matrices Q and $\mathrm{Rg}\,Q$ for particles of any shape are given in Ref. 19. The formulas become much simpler for rotationally symmetric particles provided that the axis of particle symmetry coincides with the z axis of the coordinate system. Specifically, all surface integrals then reduce to single integrals over the polar angle, and the T matrix becomes diagonal with respect to the indices m and m':[19]

$$T^{ij}_{mnm'n'} = \delta_{mm'}\, T^{ij}_{mnmn'}, \tag{29}$$

so that each mth submatrix of the T matrix can be computed separately. This significant simplification explains why nearly all numerical results obtained with the T-matrix approach pertain to bodies of revolution. Accordingly, the T-matrix codes described in Sec. 7 are specifically designed for computing light scattering by rotationally symmetry particles.

4. NUMERICAL CALCULATION OF THE T MATRIX

Explicit closed-form analytical equations for computing the T-matrix elements for rotationally symmetric particles are given in Sec. 3.5.4 of Ref. 19. Although in principle the size of the T matrix is infinite [$n_{max} = \infty$ in Eqs. (18)–(21)], in practical computer calculations the T matrix must be truncated to a finite size. The convergence size of the T matrix is determined by increasing n_{max} in unit steps until the optical cross sections and the expansion coefficients α^l_1 to β^l_2 converge within some specified accuracy. The convergence procedure described in detail in Ref. 3 produces two numbers, n_{max} and $n^1_{max} \leq n_{max}$. The first of these numbers specifies the size of the matrix Q in computing the inverse matrix Q^{-1} in Eq. (28), while n^1_{max} determines the size of the numerically significant upper left submatrix of the T matrix which is subsequently used in computing the optical cross sections and the expansion coefficients in Eqs. (11)–(16).

Since different elements of the matrix Q can differ by many orders of magnitude, the calculation of the inverse matrix Q^{-1} is an ill-conditioned process negatively influenced by round-off errors. This means that even small numerical errors in the computed elements of the matrix Q may result in large errors in the elements of the inverse matrix Q^{-1}. The round-off errors become increasingly significant with increasing particle size parameter and/or aspect ratio and rapidly accumulate with increasing size of the matrix Q. As a result, for large and/or highly aspherical particles, for which n_{max} must be large, T-matrix computations can become poorly convergent or even divergent.[20] We have shown in Ref. 4 that an efficient way of dealing with this numerical instability is to compute and invert the matrix Q using extended precision (REAL*16 and COMPLEX*32) instead to double-precision (REAL*8 and COMPLEX*16) floating-point FORTRAN variables. Furthermore, Wielaard et al[6] have found that the computation of the inverse matrix Q^{-1} for nonabsorbing and weakly absorbing particles (imaginary part of the refractive index less than about 0.001) should be based on a special form of the LU-factorization[25,26] rather than on the traditional Gauss elimination with partial pivoting,[20–22] thereby significantly increasing the maximum convergent particle size.

The calculation of the elements of the Q and $\mathrm{Rg}Q$ matrices requires a numerical evaluation of surface integrals, which, for rotationally symmetric particles, reduce to single integrals of the type

$$\int_0^\pi \mathrm{d}\theta \sin\theta f(\theta), \tag{30}$$

where θ is the polar angle. These integrals are evaluated by means of the Gauss quadrature:

$$\int_0^\pi \mathrm{d}\theta \sin\theta f(\theta) \approx \sum_{k=1}^{N_G} w_k \sin\theta_k f(\theta_k), \tag{31}$$

where θ_k and w_k are quadrature division points and weights on the interval $[0, \pi]$, respectively. The order of the quadrature N_G is increased until the convergence criterion described in Ref. 3 is fulfilled. The initial value of N_G is usually chosen as a multiple of n_{max}, the integer multiplicity factor being an important numerical parameter which should be individually optimized for each particle shape (Secs. 7 and 8).

For particles with a plane of symmetry perpendicular to the axis of rotation, the integrals over the interval $[0, \pi]$ reduce to integrals over the semi-interval $[0, \pi/2]$, and half of the integrals vanish, thereby significantly speeding up computer calculations.[20,21] Furthermore, the numerical stability and accuracy of T-matrix computations for finite circular cylinders can be greatly enhanced by dividing the integration interval $[0, \pi/2]$ into two subintervals $[0, \arctan(D/L)]$ and $[\arctan(D/L), \pi/2]$, where D is the cylinder diameter and L is the cylinder length, and applying separate Gaussian quadrature formulas to each of the two subintervals.[5,21] The codes described in Sec. 7 specifically exploit these features of the T-matrix method.

5. PARTICLE SHAPES AND SIZES

Although the T matrix codes described below can be easily tuned to any rotationally symmetric particle having a plane of symmetry perpendicular to the axis of rotation, the current versions of the codes are directly applicable to spheroids, finite circular cylinders, and even-order Chebyshev particles. Spheroids are formed by rotating an ellipse about its minor (oblate spheroid) or major (prolate spheroid) axis (Fig. 1). Their shape in the spherical coordinate system is described by the equation

$$r(\theta, \phi) = a\left[\sin^2\theta + \frac{a^2}{b^2}\cos^2\theta\right]^{-1/2}, \tag{32}$$

where θ is the polar angle, ϕ is the azimuth angle, b is the rotational (vertical) semi-axis, and a is the horizontal semi-axis. The shape and size of a spheroid can be conveniently specified by the axial ratio a/b and the radius of a sphere having the same surface area, r_s. The axial ratio is greater than 1 for oblate spheroids, smaller than 1 for prolate spheroids, and equal to 1 for spheres. Alternatively, one may use the axial ratio and the radius of a sphere having the same volume, r_v.

Similarly, the shape and size of a finite circular cylinder (Fig. 2) can be fully specified by the ratio of the diameter to the length, D/L, and the equal-surface-area-sphere radius r_s (or the equal-volume-sphere radius r_v). Note that D/L is smaller than 1 for prolate cylinders, equal to 1 for compact cylinders, and greater than 1 for oblate cylinders.

Chebyshev particles are obtained by continuously deforming a sphere by means of a Chebyshev polynomial of degree n.[20] Their shape in the spherical coordinate system is given by

$$r(\theta, \phi) = r_0[1 + \varepsilon T_n(\cos\theta)], \quad |\varepsilon| < 1, \tag{33}$$

where r_0 is the radius of the unperturbed sphere, ε is the deformation parameter, and $T_n(\cos\theta) = \cos n\theta$ is the Chebyshev polynomial of degree n (Fig. 3). All Chebyshev particles with $n \geq 2$ become partially concave as the absolute value of the deformation parameter increases and exhibit surface roughness in the form of waves running completely around the particle. Since the number of waves increases linearly with increasing parameter n, it can be called the waviness
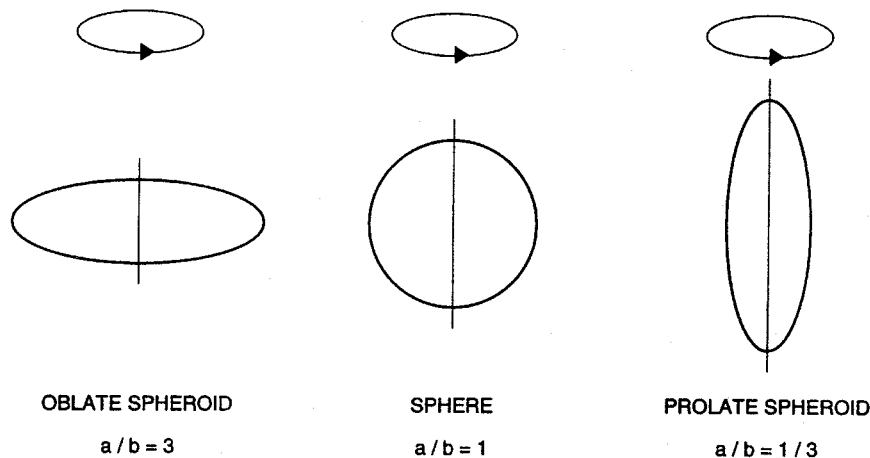

OBLATE SPHEROID   SPHERE   PROLATE SPHEROID

a / b = 3   a / b = 1   a / b = 1 / 3

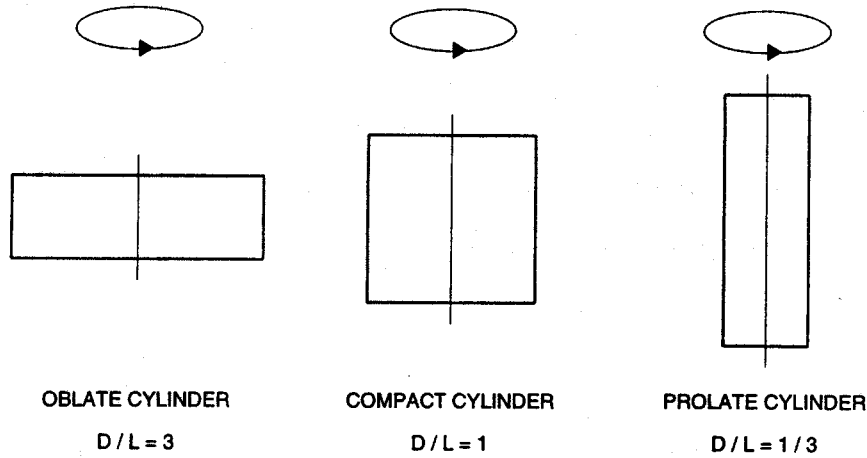Fig. 1. Spheroids with varying axial ratios.

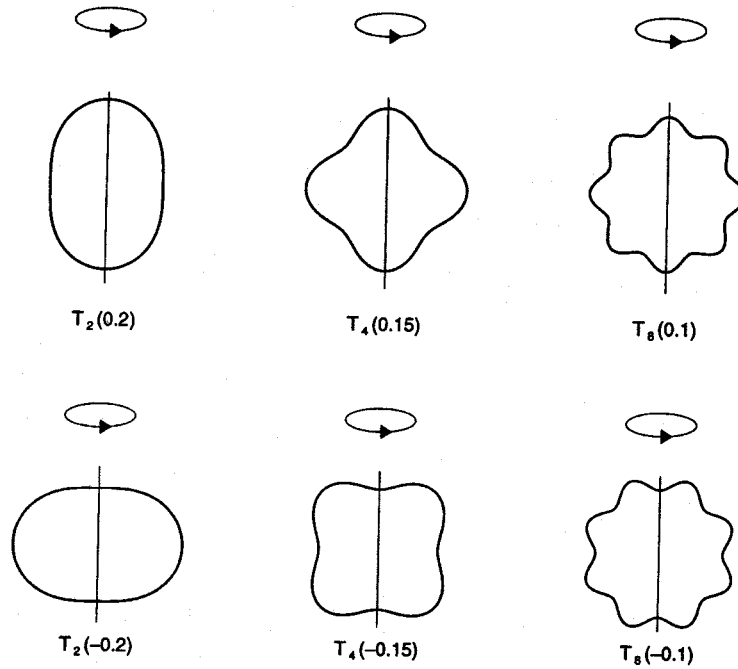Fig. 2. Circular cylinders with varying diameter-to-length ratios.

Fig. 3. Chebyshev particles $T_n(\varepsilon)$, where T_n is the *n*th Chebyshev polynomial and ε is the deformation parameter.

parameter. The shape and size of Chebyshev particles can be conveniently specified by the couple (ε, r_s) [or (ε, r_v)].

6. AVERAGING OVER SIZE DISTRIBUTION

To average the optical cross sections and the expansions coefficients in Eqs. (11)–(16) over a size distribution, one must evaluate numerically the following integrals:

$$C_{\text{sca}} = \int_{r_1}^{r_2} dr\, n(r) C_{\text{sca}}(r), \tag{34}$$

$$C_{\text{ext}} = \int_{r_1}^{r_2} dr\, n(r) C_{\text{ext}}(r), \tag{35}$$

$$\alpha_i^l = \frac{1}{C_{\text{sca}}} \int_{r_1}^{r_2} dr\, n(r) C_{\text{sca}}(r) \alpha_i^l(r), \quad i = 1, \dots, 4,$$ (36)

$$\beta_i^l = \frac{1}{C_{\text{sca}}} \int_{r_1}^{r_2} dr\, n(r) C_{\text{sca}}(r) \beta_i^l(r), \quad i = 1, 2,$$ (37)

where $n(r)\, dr$ is the fraction of particles with equivalent-sphere radii between r and $r + dr$, and r_1 and r_2 are the minimal and the maximal equivalent-sphere radii in the size distribution. The distribution function $n(r)$ is normalized to unity as follows:

$$\int_{r_1}^{r_2} dr\, n(r) = 1.$$ (38)

The integrals in Eqs. (34)–(37) are evaluated using a Gaussian quadrature formula on the interval $[r_1, r_2]$. The order of the quadrature formula depends on the size distribution and should be increased until the optical cross sections and the expansion coefficients converge.

Several convenient analytical functions are often used to model natural particle size distributions, in particular the so-called gamma distribution

$$n(r) = \frac{1}{ab\,\Gamma\!\left(\dfrac{1-2b}{b}\right)} \left(\frac{r}{ab}\right)^{(1-3b)/b} \exp\!\left(-\frac{r}{ab}\right),$$ (39)

the modified gamma distribution

$$n(r) = \frac{\gamma}{r_c \Gamma\!\left(\dfrac{\alpha+1}{\gamma}\right)} \left(\frac{\alpha}{\gamma}\right)^{(\alpha+1)/\gamma} \left(\frac{r}{r_c}\right)^{\alpha} \exp\!\left[-\frac{\alpha}{\gamma}\left(\frac{r}{r_c}\right)^{\gamma}\right],$$ (40)

the log normal distribution

$$n(r) = \frac{1}{(2\pi)^{1/2} r \ln \sigma_g} \exp\!\left[-\frac{(\ln r - \ln r_g)^2}{2\ln^2 \sigma_g}\right]$$ (41)

with $\sigma_g > 1$, and the power law size distribution[27]

$$n(r) = \begin{cases} \dfrac{2r_1 r_2}{r_2^2 - r_1^2} r^{-3} & \text{for } r_1 \le r \le r_2, \\[2ex] 0 & \text{otherwise.} \end{cases}$$ (42)

Important characteristics of a size distribution are the effective radius r_{eff} and effective variance v_{eff} defined as[27]

$$r_{\text{eff}} = \frac{1}{G} \int_{r_1}^{r_2} dr\, r \pi r^2 n(r),$$ (43)

$$v_{\text{eff}} = \frac{1}{G r_{\text{eff}}^2} \int_{r_1}^{r_2} dr (r - r_{\text{eff}})^2 \pi r^2 n(r),$$ (44)

where

$$G = \int_{r_1}^{r_2} dr\, \pi r^2 n(r).$$ (45)

Although the mathematical value of the parameter r_2 for the gamma, modified gamma, and log normal distributions is infinity, a finite value must be chosen in practical computer calculations. Two interpretations of a truncated size distribution can be given. First, r_2 can be increased until the scattering cross sections and the expansion coefficients converge within some numerical accuracy. In this case the converged truncated size distribution is numerically equivalent to the distribution with $r_2 = \infty$. Second, a truncated distribution can be considered a specific distribution with optical cross sections, expansion coefficients, effective radius, and effective variance different from those for the

distribution with $r_2 = \infty$. Similar considerations apply to the parameter r_1 whose mathematical value for the gamma, modified gamma, and log normal distributions is zero, but in practice can be any number smaller than r_2.

7. COMPUTER CODES

Two FORTRAN T-matrix codes for computing light scattering by polydisperse, randomly oriented, rotationally symmetric particles are available on the World Wide Web at http://www.giss.nasa.gov/~crmim. The first code uses only double-precision floating point variables, while the second one computes the T matrix elements using extended-precision floating point variables. The extended precision code is slower than the double-precision code, especially on supercomputers, but allows computations for substantially larger particles. Both codes assume that scattering particles have a plane of symmetry perpendicular to the rotational axis and are directly applicable to spheroids, finite circular cylinders, and even-order Chebyshev particles. The codes may be used without limitations in any not-for-profit scientific research provided that the source of the codes is properly acknowledged.

7.1. Input code parameters

ICHOICE:

> If ICHOICE = 1, then the code computes the inverse matrix Q^{-1} (Sec. 4) using the LU-factorization technique.[6] If ICHOICE = 2, the inverse matrix is computed using a standard Gauss elimination procedure. The CPU time in both cases is roughly the same, but the LU-factorization procedure allows computations for significantly larger particles in the case of weak or no absorption (small or zero imaginary part of the refractive index).[6]

RAT:

> If RAT = 1, the size of the particles is specified in terms of the equal-volume sphere radius r_v. If RAT $\neq$ 1, the size of the particles is specified in terms of the surface-equivalent-sphere radius r_s.

NDISTR, AXI, B, GAM, NPNAX, AXMAX:

> The parameter NDISTR specifies the particle size distribution. For the modified gamma distribution [Eq. (40)], NDISTR = 1, AXI = α, B = r_c, and GAM = γ. For the log normal distribution [Eq. (41)], NDISTR = 2, AXI = r_g, B = $\ln^2 \sigma_g$, and GAM is ignored. For the power-law distribution [Eq. (42)], NDISTR = 3, AXI = r_{eff}, B = v_{eff}, and GAM is ignored. In this case the parameters R1 and R2 (see below) are calculated from Eqs. (42)–(45) for given r_{eff} and v_{eff}. Finally, for the gamma distribution [Eq. (39)], NDISTR = 4, AXI = a, B = b, and GAM is ignored.
>
> Note that the codes compute NPNAX size distributions of the same type and with the same values of B (and GAM for NDISTR = 1) in one run. The parameter AXI varies from AXMAX down to AXMAX/NPNAX in steps of AXMAX/NPNAX. If only one size distribution is needed, set NPNAX = 1 and AXMAX equal to AXI of this size distribution.

R1 and R2:

> R1 = r_1 and R2 = r_2 are the minimal and the maximal radii of the size distribution (Sec. 6). They are calculated automatically for the power-law distribution with given AXI and B, but must be specified for other distributions after the statements
>
> DO 600 IAX = 1, NPNAX
>   AXI = AXMAX–DAX*FLOAT(IAX – 1)
> in the main program.

NKMAX:

> NKMAX is an integer such that NKMAX + 2 is the number of Gaussian quadrature points used in integrating over particle sizes in Eqs. (34)–(37) for particles with AXI = AXMAX.

For particles with AXI = AXMAX–AXMAX/NPNAX, AXMAX–2*AXMAX/NPNAX etc. the number of Gaussian points linearly decreases.

LAM:

LAM $= \lambda$ is the wavelength of the incident light. Note that $\lambda, r_c, r_g, r_{eff}, a, r_1$ and r_2 must be in the same units of length (e.g., microns).

MRR and MRI:

MRR $= m_r$ and MRI $= m_i$ are, respectively, the real and the imaginary parts of the particle refractive index. MRI must be zero for nonabsorbing and positive for absorbing particles.

EPS and NP:

These parameters specify the shape of the particles (Sec. 5). For spheroids, NP $= -1$ and EPS $= a/b$ is the ratio of the horizontal to rotational axes. For circular cylinders, NP $= -2$ and EPS $= D/L$ is the diameter-to-length ratio. For Chebyshev particles, NP must be even and positive and is the degree of the Chebyshev polynomial n, while EPS $= \varepsilon$ is the deformation parameter.

DDELT:

This parameter specifies the desired absolute accuracy of computing the expansion coefficients in Eqs. (11)–(16) (see Ref. 3 for more details).

NPNA:

NPNA is an integer and specifies the number of equidistant scattering angles from 0 to 180° at which the scattering matrix of Eq. (1) is calculated. The corresponding scattering angles in degrees are given by $(I - 1)*180/(NPNA - 1)$, where I numbers the scattering angles. This way of selecting scattering angles can be easily modified at the beginning of subroutine MATR.

NDGS:

This integer parameter controls the initial value of the number N_G of division points in computing integrals over the particle surface [Eq. (31)]. For compact particles, the recommended value of NDGS is 2. For highly aspherical particles, larger values (NDGS $= 3, 4, \dots$) may be necessary to obtain convergence (Sec. 8). Although the codes check convergence over the number of Gauss division points N_G in Eq. (31), they do not check convergence over the initial value of N_G which depends on the choice of NDGS. Therefore, false convergence can be obtained in some cases, especially for highly elongated or flattened particles, and control comparisons of results obtained with different NDGS-values are recommended.

7.2. Output code parameters

REFF and VEFF:

REFF $= r_{eff}$ and VEFF $= v_{eff}$ are the effective radius and effective variance of the size distribution defined by Eqs. (43)–(45).

CEXT and CSCA:

CEXT $= C_{ext}$ and CSCA $= C_{sca}$ are the extinction and scattering cross sections per particle. Their dimension is that of λ squared. For example, if $\lambda, r_c, r_g, r_{eff}, a, r_1$, and r_2 are given in microns, then the cross sections are computed in square microns.

W:

W $= \varpi$ is the single scattering albedo.

$\langle \cos \rangle$:

$\langle \cos \rangle = g$ is the asymmetry parameter of the phase function.

F11, ... , F44:

F11 $= a_1(\Theta)$, ... , F44 $= b_2(\Theta)$ are the elements of the scattering matrix of Eq. (1).

LMAX1:

LMAX1 $= l_{max} + 1$ is the total number of numerically significant expansion coefficients in Eqs. (11)–(16).

ALPH1, ... , BET2:

These arrays contain the respective expansion coefficients α_1^l, ... , β_2^l and are fully computed when the statement CALL MATR appears in the main program. Note that an lth expansion coefficient is given by the $(l + 1)$th element of the respective array.

7.3. Additional comments and recipes

The physical correctness of the computed results is tested using inequalities derived by van der Mee and Hovenier.[28] Although the message that the test of van der Mee and Hovenier is satisfied does not guarantee that the results are absolutely correct, the message that the test is not satisfied means that the results may be wrong.

The CPU time consumption rapidly increases with increasing ratio radius/wavelength and/or with increasing particle asphericity. This should be taken into account in planning massive computations. The use of an optimizing compiler on IBM RISC workstations has been found to save about 70% of CPU time.

Execution can be automatically terminated if dimensions of certain arrays are not large enough. In all cases, a message appears explaining the cause of termination. The message WARNING: NGAUSS = NPNG1 means that convergence over the parameter N_G [Eq. (31); see also Ref. 3] cannot be obtained for the NPNG1 value specified in the PARAMETER statement. Often this is not a serious problem, especially for compact particles. Larger and/or more aspherical particles may require larger values of the parameters NPN1, NPN4, and NPNG1. These parameters must be changed simultaneously in the main program and all subroutines. It is recommended that the relations NPN1 = NPN4 + 25 and NPNG1 = (NDGS + 1)*NPN1 be maintained. Note that the memory requirement increases as the third power of NPN4. If the memory of a computer is too small to accommodate the code with its current setting, the parameters NPN1, NPN4, and NPNG1 can be reduced simultaneously in the main program and all subroutines. However, this will decrease the maximum particle size that can be handled by the code.

In some cases any increases of NPN1 will not make the T-matrix computations convergent. This means that the particle is just too extreme in size parameter and/or aspect ratio for given refractive index. The main program contains several PRINT statements which are currently commented out. If uncommented, these statements will produce numbers which show the convergence rate and can be used to determine whether T-matrix computations for given particle parameters will converge at all.

The recommended value of the parameter DDELT is 0.001.[3] For larger values, false convergence can be obtained. The message WARNING: W IS GREATER THAN 1 means that the single-scattering albedo exceeds the maximum possible value 1. If W is greater than 1 by significantly more than DDELT, this message can be an indication of numerical instability caused by extreme values of particle parameters.

Some of the common blocks are used to save memory rather than to transfer data. Therefore, if a compiler produces a warning message that the lengths of a common block are different in different subroutines, this is not a real problem.

In computations for spheres, one should use EPS = 1.000001 instead of EPS = 1. The use of EPS = 1 can cause overflows in some rare cases. To calculate scattering by monodisperse particles in random orientation, one should use the options

NPNAX = 1
AXMAX = r
B = 1D − 1
NKMAX = −1

NDISTR = 4

...

DO 600 IAX = 1, NPNAX
        AXI = AXMAX − DAX*DFLOAT(IAX − 1)
        R1 = 0.9999999*AXI
        R2 = 1.0000001*AXI

...

where r is the equivalent-sphere radius.

When there is no preference for a specific size distribution, we recommend to use the power law size distribution rather than gamma, modified gamma, and log normal distributions, because in this case convergent solution can be obtained for larger r_{eff} and v_{eff}.[29] If results for many different size distributions are required and the refractive index is fixed, then another approach can be more efficient than running these codes many times. Specifically, scattering results should be computed for monodisperse particles with sizes ranging from essentially zero to some maximum value with a small step size. These results should be stored on disk and then can be used along with spline interpolation to compute scattering by particles with intermediate sizes and numerically evaluate integrals in Eqs. (34)–(37). Scattering patterns for monodisperse nonspherical particles in random orientation are smoother than for monodisperse spheres,[7] and spline interpolation usually gives good results. In this way, averaging over any new size distributions can be a matter of a few seconds of CPU time.[5]

8. EXAMPLES

Table 1 shows the values of the maximal convergent size parameter $x_s = 2\pi r_s/\lambda$ for DDELT = 0.001 in extended-precision T-matrix computations for monodisperse oblate spheroids with refractive index 1.311 and axial ratios a/b varying from 1.5 to 20. Note that the maximal size parameter $x_a = 2\pi a/\lambda$ measured along the major semi-axis a can be significantly larger than the maximal equivalent-sphere size parameter, especially for highly flattened spheroids. Table 1 also shows the respective values of the parameter NDGS which controls the initial number of Gauss points in Eq. (31). Table 2 is analogous to Table 1, but is computed for prolate spheroids and displays the major axis size parameter $x_b = 2\pi b/\lambda$ rather than x_a. It is clear that the maximal convergent size parameters strongly depend on the spheroid axial ratio and significantly increase as the particles become less aspherical. Tables 1 and 2 also demonstrate that converged computations

Table 1. Maximal convergent size parameters x_s and x_a and NDGS versus axial ratio a/b in extended-precision calculations for monodisperse oblate spheroids with refractive index 1.311

a/b	x_s	x_a	NDGS
20	12	17	30
10	17	24	15
5	27	37	5
3	42	54	4
2	92	111	3
1.5	>160	>180	2

Table 2. Maximal convergent size parameters x_s and x_b and NDGS versus axial ratio a/b in extended-precision calculations for monodisperse prolate spheroids with refractive index 1.311

a/b	x_s	x_b	NDGS
0.05	3	15	30
0.1	7	25	25
0.2	14	35	10
0.333	30	57	5
0.5	73	112	2
0.667	>150	>194	2

Table 3. Maximal convergent size parameters x_s and x_a and NDGS versus refractive index in extended-precision calculations for monodisperse oblate spheroids with axial ratio $a/b = 3$

Refractive index	x_s	x_a	NDGS
1.311	42	54	4
1.53 + 0.008i	38	48	4
1.78 + 0.005i	32	41	4
2 + 0.6i	25	32	4

Table 4. Maximal convergent size parameter x_s versus axial ratio a/b in different types of T-matrix computations for monodisperse oblate spheroids with refractive index 1.311

a/b	Extended precision, LU-factorization	Double precision, LU-factorization	Double precision, Gauss elimination
20	12	4	4
15	13	6	4
10	17	7	5
5	27	12	7
3	42	19	10
2	92	38	14
1.5	>160	97	24

Table 5. Maximal convergent size parameter x_s versus diameter-to-length ratio D/L in different types of T-matrix computations for monodisperse oblate cylinders with refractive index 1.311

a/b	Extended precision, LU-factorization	Double precision, LU-factorization	Double precision, Gauss elimination
20	7	1.5	0.8
15	7	1.5	0.9
10	13	3	0.9
5	24	10	1.2
3	43	17	5
2	70	30	12
1.5	>150	93	21

for highly flattened and elongated spheroids may require large values of the parameter NDGS. Table 3 shows that the maximal convergent size parameters also depend on the particle refractive index and can significantly decrease with increasing real and/or imaginary parts of the refractive index. Table 4 clearly demonstrates the advantage of using extended-precision instead of double-precision arithmetic and using the special LU-factorization-based matrix inversion procedure in place of the traditional Gauss elimination scheme with partial pivoting. Finally, comparison of Tables 4 and 5 shows that although cylinders are particles with edges, they can be treated using the T-matrix codes almost as successfully as smooth spheroids with a similar aspect ratio.

As an example of T-matrix computations for particles with a large axial ratio and a large size parameter, Figs. 4 and 5 depict the elements of the scattering matrix for two models of monodisperse, randomly oriented oblate spheroids with refractive index 1.311. Figure 4 is computed for the axial ratio $a/b = 20$ and surface-equivalent-sphere size parameter $x_s = 12$, while Fig. 5 is computed for $a/b = 1.5$ and $x_s = 130$. The computations were performed on an IBM RISC model 39H workstation and took 4.5 min of CPU time for the first model and 8 hours for the second model.

9. CONCLUSIONS

Predecessors of the T-matrix codes described in this paper have been extensively used by members of the scattering community since 1993. Multiple communications with the users provided a positive feedback which helped us to improve the codes and suggested the idea of publishing a detailed user guide collecting in one place all key formulas and describing the basics of the
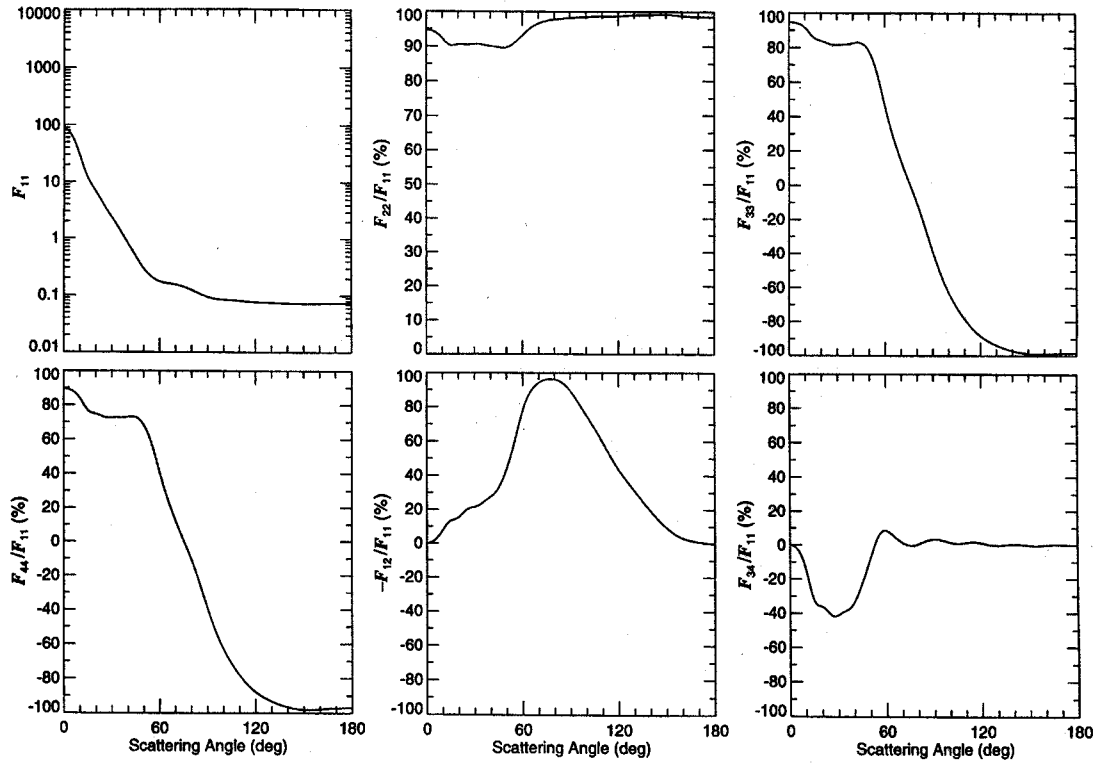
Fig. 4. Elements of the scattering matrix for randomly oriented oblate spheroids with refractive index 1.311, axial ratio $a/b = 20$, and surface-equivalent-sphere size parameter $x_s = 12$.
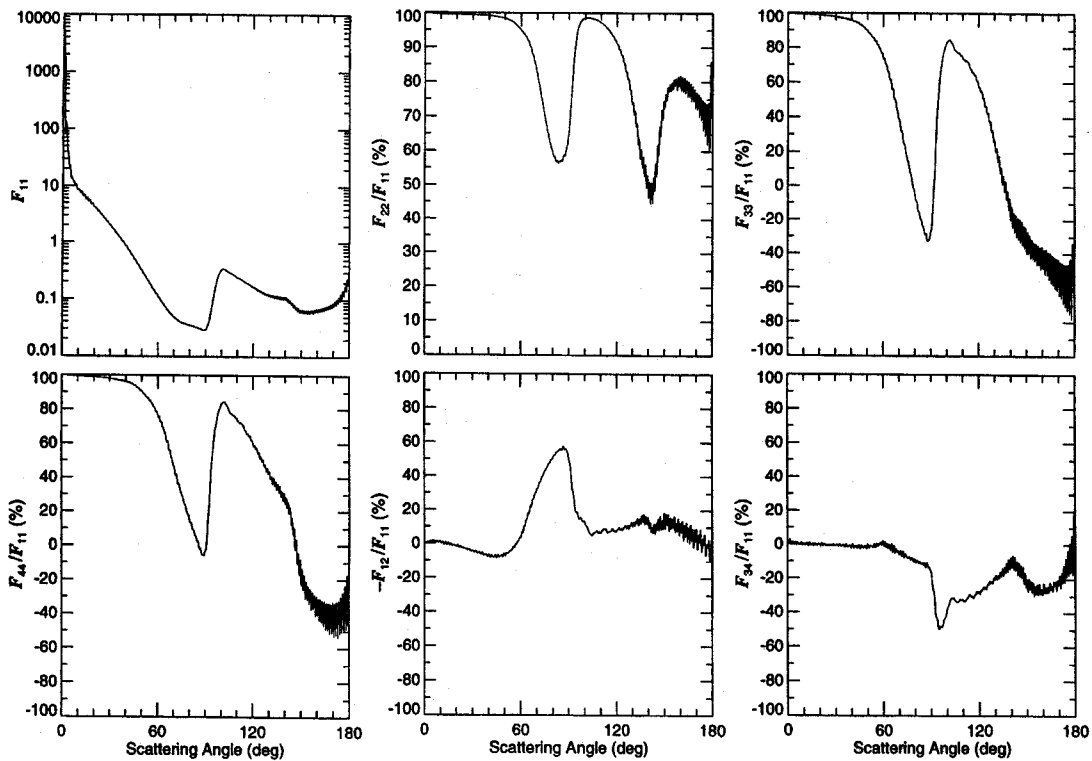

Fig. 5. As in Fig. 4, but for $a/b = 1.5$ and $x_s = 130$.

approach, numerical aspects of computer calculations, and the capabilities and limitations of the technique. We hope, therefore, that this paper can serve a useful purpose.

Due to the high speed and accuracy of the extended boundary condition method and its applicability to particles with very large size parameters and aspect ratios (Sec. 8), and also due to the use of the highly efficient analytical method for computing orientationally averaged optical cross sections and scattering matrix elements,[2] our T-matrix codes may be the most powerful tool for computing the scattering of light by randomly oriented rotationally symmetric particles based on directly solving Maxwell's equations. Furthermore, the codes have been found to be able to produce very accurate results (five and more exact decimal places) suitable for use as benchmarks.[2,5,6] It is important that unlike many other techniques, our codes have an automatic built-in convergence test which provides a very good estimate of the absolute accuracy of T-matrix computations.[30]

An obvious disadvantage of our codes is that they are applicable only to bodies of revolution such as spheroids, finite circular cylinders, and Chebyshev particles. However, by varying the spheroid axial ratio or the cylinder diameter-to-length ratio one can specify a wide variety of smooth and sharp-edged nonspherical shapes ranging from needles to plates and thus, model light scattering by convex bodies with major deviations of the shape from that of a sphere. On the other hand, the best application for Chebyshev particles is a study of the effect of surface roughness and mild concavity on surfaces of nearly spherically shaped particles. It should also be noted that several attempts have already been made to use the T-matrix method in computations for particles without rotational symmetry.[31-35]

All these features should make the T-matrix codes the first choice in those cases when the scattering particles are clearly nonspherical and Mie theory can be expected to produce inadequate results. The T-matrix codes are so much faster than all other available techniques that it is reasonable to try them first before deciding that modeling of scattering properties of nonspherical particles in the framework of a specific application indeed necessitates switching to alternative approaches such as the discrete dipole approximation[36-39] or the finite difference time domain method.[40,41] It should be remembered that although the latter techniques are applicable to arbitrarily shaped particles, they are significantly less accurate (especially in computations of the scattering matrix rather than just the optical cross sections) and are limited to much smaller size parameters.

REFERENCES

1. Waterman, P. C., *Phys. Rev. D*, 1971, **3**, 825–839.
2. Mishchenko, M. I., *J. Opt. Soc. Am. A*, 1991, **8**, 871–882; errata 1992, **9**, 497.
3. Mishchenko, M. I., *Appl. Opt.*, 1993, **32**, 4652–4666.
4. Mishchenko, M. I. and Travis, L. D., *Opt. Comm.*, 1994, **109**, 16–21
5. Mishchenko, M. I., Travis, L. D. and Macke, A., 1996, *Appl. Opt.*, **35**, 4927–4940.
6. Wielaard, D. J., Mishchenko, M. I., Macke, A. and Carlson, B. E. *Appl. Opt.*, 1997, **36**, 4305–4313.
7. Mishchenko, M. I., Travis, L. D. and Mackowski, D. W., *J. Quant. Spectrosc. Radiat. Transfer*, 1996, **55**, 535–575.
8. van de Hulst, H. C., *Light Scattering by Small Particles*. Wiley, New York, 1957.
9. Bohren, C. F. and Huffman, D. R., *Absorption and Scattering of Light by Small Particles*. Wiley, New York, 1983.
10. Mishchenko, M. I. and Hovenier, J. W., *Opt. Lett.*, 1995, **20**, 1356–1358.
11. de Haan, J. F., Bosma, P. B. and Hovenier, J. W., *Astron. Astrophys.*, 1987, **183**, 371–391.
12. Gelfand, I. M., Minlos, R. A. and Shapiro, Z. Ya., *Representations of the Rotation and Lorentz Groups and their Applications*. Pergamon Press, Oxford, 1963.
13. Hovenier, J. W. and van der Mee, C. V. M., *Astron. Astrophys.*, 1983, **128**, 1–16.
14. Kuščer, I. and Ribarič, M., *Opt. Acta*, 1959, **6**, 42–51.
15. Sobolev, V. V., *Light Scattering in Planetary Atmospheres*. Pergamon Press, Oxford, 1974.
16. van de Hulst, H. C., *Multiple Light Scattering. Tables, Formulas, and Applications*. Academic Press, San Diego, 1980.
17. Lenoble, J., ed., *Radiative Transfer in Scattering and Absorbing Atmospheres: Standard Computational Procedures*. Deepak, Hampton, VA, 1985.

18. Yanovitskij, E. G., *Light Scattering in Inhomogeneous Atmospheres*. Springer, Berlin, 1997.
19. Tsang, L., Kong, J. A. and Shin, R. T., *Theory of Microwave Remote Sensing*, Wiley, New York, 1985.
20. Wiscombe, W. J. and Mugnai, A., NASA Ref. Publ. 1157, NASA/GSFC, Greenbelt, MD, 1986.
21. Barber, P. W. and Hill, S. C., *Light Scattering by Particles: Computational Methods*. World Scientific, Singapore, 1990.
22. Sid'ko, F. Ya., Lopatin, V. N. and Paramonov, L. E., *Polarization Characteristics of Suspensions of Biological Particles*. Nauka, Novosibirsk, 1990 (in Russian).
23. Wauben, W. M. F., private communication, 1993.
24. Barber, P. and Yeh, C., *Appl. Opt.*, 1975, **14**, 2864–2872.
25. Golub, G. H. and van Loan, C. F., *Matrix Computations*. John Hopkins Univ. Press, Baltimore, MD, 1989.
26. *NAG Fortran Library Manual, Mark 15*. The Numerical Algorithms Group Ltd., Oxford, UK, 1991.
27. Hansen, J. E. and Travis, L. D., *Space Sci. Rev.*, 1974, **16**, 527–610.
28. van der Mee, C. V. M. and Hovenier, J. W., *Astron. Astrophys.*, 1990, **228**, 559–568.
29. Mishchenko, M. I. and Travis, L. D., *Appl. Opt.*, 1994, **33**, 7206–7225.
30. Hovenier, J. W., Lumme, K., Mishchenko, M. I., Voshchinnikov, N. V., Mackowski, D. W. and Rahola, J., *J. Quant. Spectrosc. Radiat. Transfer*, 1996, **55**, 695–705.
31. Schneider, J. B. and Peden, I. C., *IEEE Trans. Antennas Propag.*, 1988, **36**, 1317–1321.
32. Schneider, J. B., Brew, J. and Peden, I. C., *IEEE Trans. Geosci. Remote Sens.*, 1991, **29**, 555–562.
33. Wriedt, T. and Doicu, A., *J. Mod. Opt.*, 1998, **45**, 199–213.
34. Laitinen, H. and Lumme, K., *J. Quant. Spectrosc. Radiat. Transfer*, 1998, this issue.
35. Wriedt, T., *J. Quant. Spectrosc. Radiat. Transfer*, 1998, this issue.
36. Draine, B. T. and Flatau, P. J., *J. Opt. Soc. Am. A*, 1994, **11**, 1491–1499.
37. Lumme, K. and Rahola, J., *Astrophys. J.*, 1994, **425**, 653–667.
38. Hoekstra, A. G. and Sloot, P. M. A., in *Proceedings of the 1st Workshop on Electromagnetic and Light Scattering—Theory and Applications*, ed. T. Wriedt, M. Quinten and K. Bauckhage, Universität Bremen, Bremen, 1996, pp. 7–18.
39. Lumme, K., Rahola, J. and Hovenier, J. W., *Icarus*, 1997, **126**, 455–469.
40. Kunz, K. S. and Luebbers, R. J., *The Finite Difference Time Domain Method for Electromagnetics*, CRC Press, Boca Raton, FL, 1993.
41. Yang, P. and Liou, K. N., *J. Opt. Soc. Am. A*, 1996, **13**, 2072–2085.